ARCHIVES
of
FOUNDRY ENGINEERING

ISSN (2299-2944)
Volume 2024
Issue 3/2024

94 – 100

14/3

10.24425/afe.2024.151297

Published quarterly as the organ of the Foundry Commission of the Polish Academy of Sciences

Effect of Span-80 to Moisture Resistance of Near-infrared Curing 3D Printing Sodium Silicate Foundry Sands

Ao Xue [a], Yuhan Tang [a], Yao Li [b], Weihong Dai [a], Jijun Lu [a], Huafang Wang [a] *

[a] School of Mechanical Engineering and Automation, Wuhan Textile University, China
[b] Dongfeng Motor Corporation Research & Development Institute, China
* Corresponding author. E-mail address: wanghfhust@163.com

Received 15.05.2024; accepted in revised form 02.09.2024: available online 11.10.2024

Abstract

In this work, a new method of near-infrared curing 3D printing sodium silicate sands (NIRC3DPSSS) driven by photovoltaic cells was proposed, and the Span-80 moisture resistance modifier was studied. NIRC3DPSSS had the advantages of high strength, rapid curing and low residual strength. However, the 24h storage strength would reduce because Na^+ in the bonding bridges could absorb moisture. The experimental results showed that the strength of Span-80 modified sands molds reached 0.95MPa after 4 hours in a humidistat with 99%RH (relative humidity) containing 2.2% sodium silicate, an increase of 97.9% comparing to common sands molds. In air(80%RH), the strength reached 1.25MPa, an increase of 40.4%. The optimal effect of modification was achieved when Span-80 was 0.066% of the raw sands. Additionally, the bonding film and bridges in sodium silicate sands modified with Span-80 were more stable, smoother and free of cracks when observed using scanning electron microscopy (SEM) and energy dispersive spectroscopy(EDS).

Keywords: Sodium silicate sands, Span-80, Near-infrared curing 3D printing, Moisture resistance

1. Introduction

Sodium silicate, an effective and eco-friendly inorganic chemical binder, is widely used across various sectors due to its cost-effectiveness and fluidity. However, most sodium silicate sands processes still relied on manual molding, which was time-consuming and challenging for complex-shaped castings. Conventional curing methods for sodium silicate sands included carbon dioxide, organic ester, microwave and thermal curing. Carbon dioxide-cured sands molds with 8% sodium silicate exhibited poor collapsibility and reusage; organic ester curing with 4% sodium silicate was slow; microwave and thermal cured molds with 3% sodium silicate were faster but consumed more energy and exhibited poor moisture resistance [1-2].

Casting sands 3D printing was widely adopted [3-4]. In 1990, Sachs et al. pioneered the use of micro-droplet jetting technology to bond aluminum oxide powder layer-by-layer with a sol-gel, successfully creating ceramic shells and cores [5]. Z Corp in the United States developed a process for ceramic shells, using proprietary starch-based and gypsum-based powders, mainly for casting non-ferrous metals. Generis in Germany developed GS process, primarily for quick sands mold manufacturing. It started with spraying binder on powder layer, then selectively spraying catalyst to cure the sands, complicating cleaning and reducing material recycling rates. Tsinghua University and Beijing Yin Hua Laser Rapid Prototyping and Mold Technology Co., Ltd. co-developed dual-nozzle resin sands 3D printing process. One nozzle sprayed furan resin, the other binder. This method resulted in molds with lower dimensional accuracy and high gas emissions. Li Xiaoyan et al. used their micro-

jetting bonding rapid prototyping system to perform experiments with gypsum-based powders [6].Harbin Institute of Technology developed sun-tracking 3D printing platform. This system integrated Fresnel lens concentrator, powder bed actuation platform, and an auxiliary heating device to prevent sintering cracks, enabling direct sunlight powder bed fusion additive manufacturing [7-8]. Although MARKUS K produced desert sands artifacts using a direct sunlight 3D printer, the underlying research was still not in-depth [9]. As can be seen from the above, binders used for 3D printing sands molds, primarily toxic and high-emission organic resins like furan and phenolic resins, require extensive hardening or drying processes. These steps pose significant environmental hazards.

As solar technology advanced globally and the cost of photovoltaic cells dropped, photovoltaic technology had significant advantages in the global market. At the same time, NIR resistance wires could fast heat up to 1000℃, enabling uniform and rapid material heating, showed great potential in industrial production and manufacturing [10]. Utilizing solar energy to power near-infrared curing 3D printing sodium silicate sands (NIRC3DPSSS) to develop moldless, high strength, easily collapsible and recyclable sodium silicate sands became possible. Moreover, technology for improving the moisture resistance of sodium silicate sands by modifying the binder and the raw sands had matured and supported for improving material properties.

Fig.1 illustrated the molecular structure of the nonionic surfactant Span-80 (sorbitan monooleate, chemical formula: $C_{24}H_{44}O_6$) [11]. As for sodium silicate sands modified with Span-80, shorter groups penetrated the sodium silicate on the right, achieving compatibility, while longer carbon chains on the left created a hydrophobic barrier on adhesive film and bonding bridges. This barrier shielded silica sands from moisture, reducing absorption and accumulation. Thus, Span-80 could be served as moisture-proofing agent for cured sodium silicate sands [12]. Additionally, considering Span-80 decompose and release exhaust gas when casting molds, foundries in China strictly adhere to national laws and regulations for dust and gas capture, which greatly avoids the environmental pollution caused by emission of dust and exhaust gas.

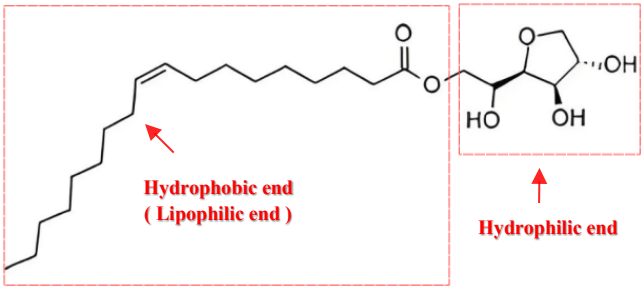

Fig.1. The molecular structure of Span-80

In this work, a new method of using photovoltaic cells to drive NIRC3DPSSS was proposed. Rapid, uniform production of sodium silicate sands molds was achieved by modifying the raw sands with the surfactant Span-80 and the curing temperature was 500℃.Molds containing 2.0%~2.6% sodium silicate demonstrated high strength, easy collapsibility and moisture resistance. The storage strength in both air with 80%RH (relative humidity) and humidistat(99%RH) was investigated. Additionally, the microstructure of the sodium silicate sands molds was observed using scanning electron microscope(SEM) and energy dispersive spectroscopy(EDS).

2. Experimental part

2.1. Material and equipment

The experimental materials comprised quartz sands with a particle size of 70/100 mesh, sodium silicate with modulus of 2.3, sodium silicate with a density of 1.48 g/ml, and a specified addition of Span-80. The sands were cured by NIR resistance wires with 1500 watts. Temperature and moisture were monitored using a TESTO 610 temperature and moisture meter, with the ambient temperature maintained at 23℃ [13-14]. A SHY vane sands mixer was employed to mix the raw sands and Span-80. Cylindrical sands molds, each measuring 30 millimeters in diameter and height (Φ30×30 mm), were semi automatically fabricated by 3D printer. Moisture was maintained at 80%RH in air and 99%RH in humidistat. The compressive strength was tested by SWQ-A material high temperature strength tester [15].

2.2. Preparation of sands molds and properties test

Fig.2 depicted the schematic diagram of solar power supplying the 3D printing mechanism. Solar panels converted sunlight into electrical energy, which was stored in photovoltaic cells. This energy was converted from 12V to 220V to drive the 3D printer via a power inverter. The electrical energy primarily facilitated the following processes: moving the sandbox and spreading powder, moving the printhead and printing layer-binder, moving the NIR resistance wires and curing sodium silicate sands, and descending the printing platform.

Fig.3 illustrated the flowchart of the manufacturing process. Raw sands and Span-80 were mixed for 2 minutes at a specific addition and then transferred to the sandbox. The sandbox spread the powder across the surface of the XY printing platform along the X-axis, followed by the printhead printing sodium silicate layer-binder at predetermined positions. The NIR resistance wires then followed the same path to scan the platform, completing the curing of the first layer. Subsequently, the platform descended a preset distance along the Z-axis, repeating the process for each layer. After a period, the molds were demolded, producing standard cylindrical specimens [16].

Fig.4 depicted NIRC3DPSSS printer system. The software component currently supported printing of sands molds, with some hardware controls under ongoing development. This system could realize semi-automatic molding.

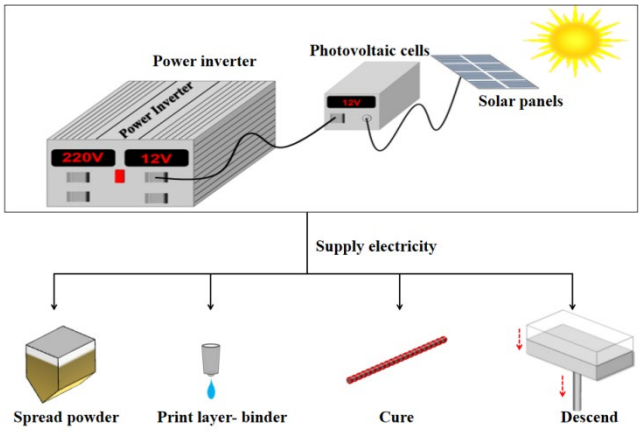

Fig. 2. The schematic diagram of solar power supplying the 3D printing mechanism

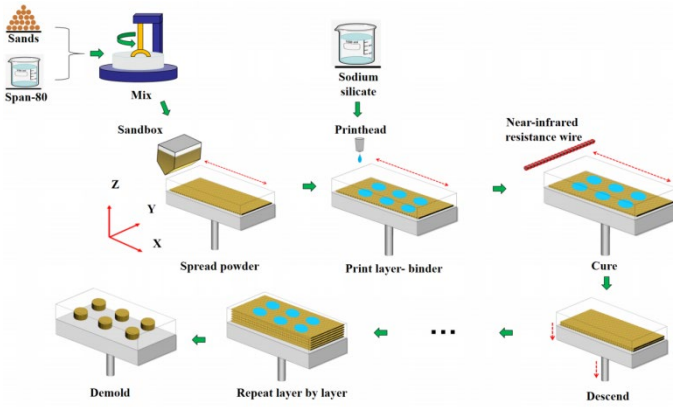

Fig. 3. The flowchart of the manufacturing process

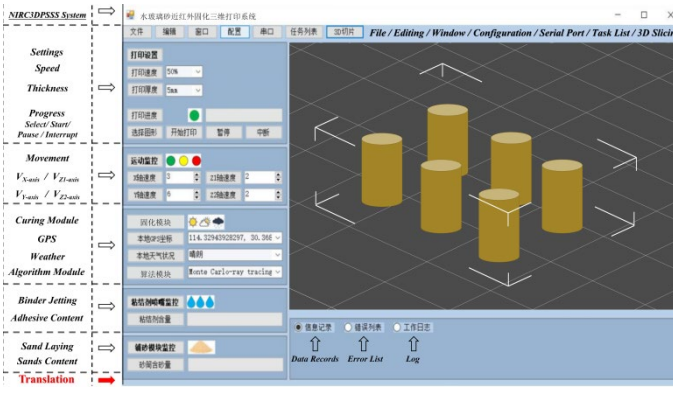

Fig. 4. NIRC3DPSSS printer system

The strength and storage strength of the sands molds after NIR curing were tested. In this work, "strength" referred to the compressive strength of sodium silicate sands immediately after curing via NIR resistance wires after 3 minutes cooling. "Storage strength" referred to the compressive strength of sodium silicate sands after being left in air (80%RH) or in humidistat (99%RH) for 4 hours. All test results were the average of six measurements.

The experiment consisted of two parts. On the one hand, 600 grams of raw sands and 12-15.6 grams of sodium silicate binder were placed into sandbox and printhead respectively, and then the sands were cured using NIR resistance wires. On the other hand, Due to the non-toxicity of Span-80, its low toxicity upon thermal decomposition, and limited solubility in organic compounds and sodium silicate, we maintained the concentration at 5% or lower. Cost considerations also played a role in this decision. Only 600 grams of raw sands and Span-80, comprising 1%, 2%, 3%, 4% and 5% of the sodium silicate binder (corresponding to 0.022%, 0.044%, 0.066%, 0.088% and 0.11% of the raw sands), were mixed in sands mixer for 2 minutes and then transferred to the sandbox. These minimal amounts ensured that Span-80 won't release substantial toxic gases during casting. 13.2 grams of sodium silicate binder, which was 2.2% of the raw sands, was added to the printhead. All experimental curing time was 12 minutes and the molds were left in air and humidistat for 4 hours.

This study investigated the effects of curing time and sodium silicate additions on strength after cooling for 3 minutes (immediate strength). The research further evaluated the strength changes being exposed in air (80%RH) and in humidistat(99%RH) for 24 hours. The effect of different Span-80 additions on the moisture resistance was investigated additionally.

3. Results and discussion

3.1. Storage strength before modification

Fig. 5 illustrated that the immediate strength of the sands molds increased with the curing time when the sodium silicate addition was 2.0%~2.6%. Molds with higher sodium silicate additions rapidly formed bonding bridges, leading to quicker strength gains and higher rate of immediate strength gains. Molds exposed to longer of NIR curing absorbed more energy, resulting in denser network structures and higher molds strength. Sodium silicate sands molds reached operational strength within about 10 minutes with NIR, much faster than organic ester curing (24 hours).

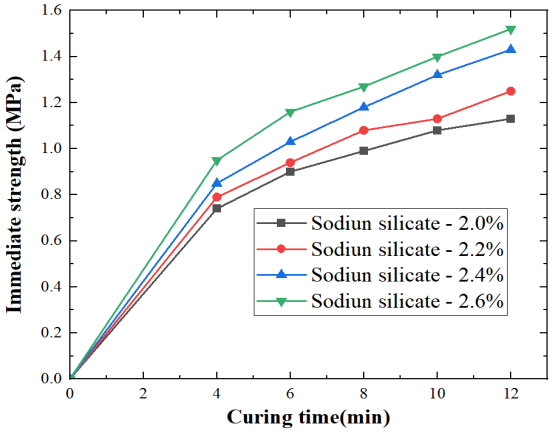

Fig. 5. Effect of curing time and sodium silicate addition on immediate strength

Fig.6 showed the effect of storage time and sodium silicate addition on the storage strength of sands molds in air (80%RH). The storage strength decreased with increasing storage time, and molds with a higher sodium silicate addition had a lower loss rates. After 2 hours of storage, the strength with 2.6% sodium silicate decreased by 7.9% comparing to immediate strength, while a 10.6 % decrease for those with 2.0% sodium silicate. After 4 hours, molds with 2.6% sodium silicate showed a 26.3% reduction in strength, while those with 2.0% experienced a 31.9%. After 24 hours, the strength with 2.6% sodium silicate was reduced by 68.4%, compared to a 88.5% for those with 2.0% .

As showed in Fig.7, sands storage strength with 2.6% sodium silicate exhibited a 16.4% reduction comparing to immediate strength while those with 2.0% reduced by 31.9% after 2 hours of storage. For 4 hours, the strength with 2.6% sodium silicate reduced by 37.5%, compared to a 64.6% reduction for those with 2.0 %. After 24 hours, the strengths were close to zero. The weakening was caused by moisture absorbed by Na^+ ions and silanol groups, which eroded the matrix, broke silicon-oxygen bonds, and increased moisture absorption, leading to dissolution and a sharp decrease in bond strength.

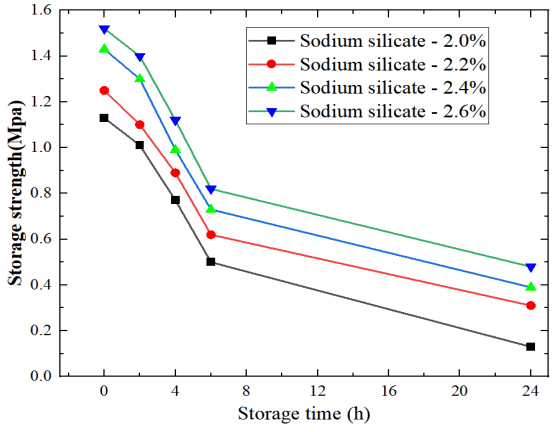

Fig. 6. Effect of storage time and sodium silicate addition on storage strength(in air,80%RH)

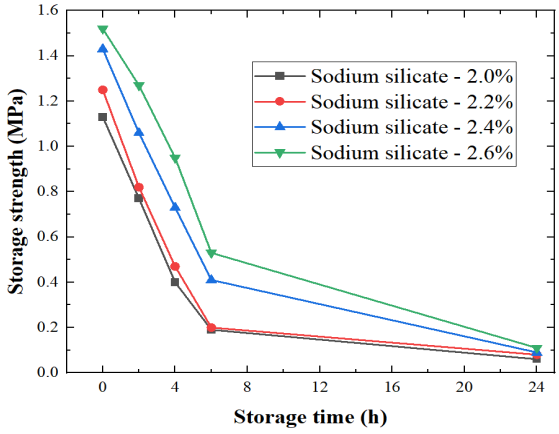

Fig. 7. Effect of storage time and sodium silicate addition on storage strength (in humidistat,99%RH)

Fig.8 provided a microscopic comparison of sands before and after moisture absorption. The cured sodium silicate bonding film and bridges, interconnected by silica-oxygen tetrahedra, formed a tightly knit 3D spatial network structure before moisture absorption (Fig.8(a)). That resulted in the sands grains being firmly bonded with high strength. Within the -Si-O-Si- network, oxygen atoms were present as bridging oxygens. Due to the moisture absorption of the Na^+, atmospheric moisture was absorbed on the surface of the sands molds. The moisture then underwent slow hydrolysis, disrupted the silica-oxygen bonds and formed microcracks. The disruption of silicon-oxygen bonds led to the formation and propagation of microcracks in the glass matrix (refer to Equation 1). As moisture absorption increased, these cracks widen and the fractures expanded (Fig.8(c)). Stress further accelerated the bond-breaking reactions, thereby compromising the inner bonding bridging oxygen system, reducing the strength of the sands molds, and undermining surface stability. Finally, the bonding film began to dissolve and the bonding bridges completely disappeared thus the strength became null (Fig.8(d)).

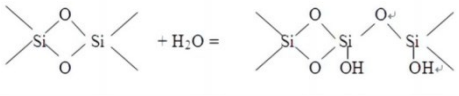

(1)

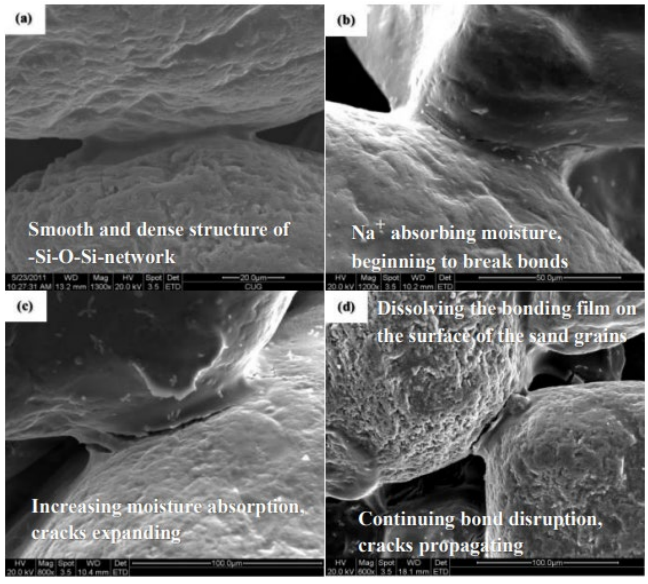

Fig. 8. Microstructure of NIRC3DPSSS bonding bridges before and after moisture absorption
a) Before moisture absorption, b) Microcracks after moisture absorption, c) Expansion cracks after moisture absorption, d) Crack penetration after moisture absorption

3.2. Storage strength after modification

The study investigated the effects of various additions of Span-80 on the storage strength of sodium silicate sands. Additionally, the microstructure of the sands modified with Span-80 was

examined, revealing how Span-80 as a modifier enhanced the moisture resistance, thereby increasing strength.

Fig.9a depicted the changes on storage strength of sodium silicate sands containing 2.2% sodium silicate, after modification with various additions of Span-80 and stored for 4 hours in both air(80%RH) and humidistat(99%RH). The results showed that sands modified with Span-80 reached 0.95MPa, exhibited 97.9% increase on storage strength in humidistat. And in air, the strength reached 1.25MPa, 40.4% increase compared to unmodified sands molds. The optimal modification effect was achieved when Span-80 was 0.066% of the raw sands.

Fig.9b and Fig.9c illustrated the changes in storage strength over time for sands containing 2.2% sodium silicate, both before and after modification with 3% Span-80, when stored in air (80% RH) and in a humidistat (99% RH). The results demonstrated that after 24 hours of storage, sands modified with 3% Span-80 retained a storage strength of approximately 0.8MPa in the humidistat and 1.1MPa in air, significantly higher than sands without Span-80. This indicated that the 3% Span-80 modification was effective and sands molds modified with Span-80 demonstrated good long-term stability and performance.

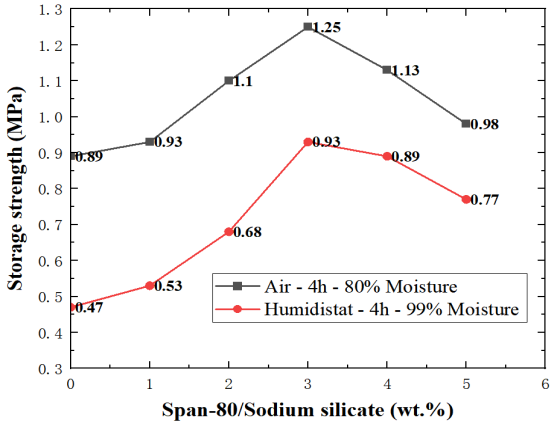

Fig. 9a. Effect of Span-80 addition on storage strength

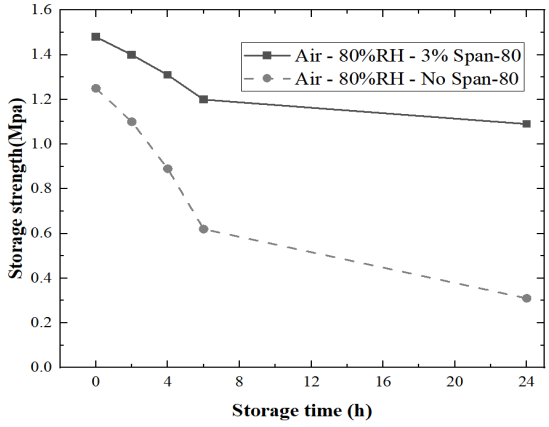

Fig. 9b. Effect of storage time and 3% Span-80 on storage strength (in air,80%RH)

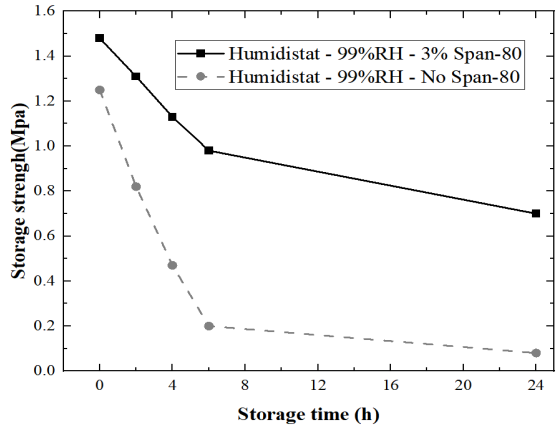

Fig. 9c. Effect of storage time and 3% Span-80 on storage strength (in humidistat,99%RH)

Fig.10 illustrated the multi-scale model of 3D printing sodium silicate sands modified with Span-80. After mixing the raw sands with Span-80 and applying sodium silicate binder, bonding film formed on the surface of the sands grains with bonding bridges developed between them. After NIR curing, the moisture within the bonding film and bridges evaporated, leading to the formation of Span-80 moisture-resistant protective film on the surface. This protective film inhibited the hygroscopic Na^+ absorbing moisture, thereby achieving effective moisture resistance.

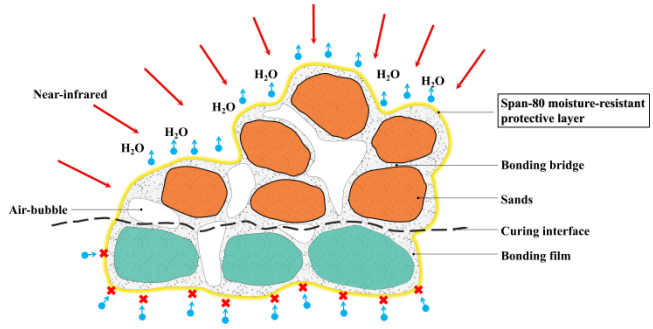

Fig. 10. Multi-scale model of NIRC3DPSSS modified with Span-80

As depicted in Fig.11, the sodium silicate bonding bridges of the unmodified sands exhibited cracks during NIR curing and storage (Fig.11(a)). The surface of the bonding bridges modified with Span-80 were smoother and devoid of cracks, resulting in higher strength (Fig.11(b)). Elemental analysis via EDS at selected locations in Fig.11(b) (refer to Table 1) indicated that the carbon content at point A exceeded that at point C (both carbon contributions were from Span-80), suggesting more Span-80 on the the surface of bonding bridges. Point B might represent undissolved Span-80.

As depicted in Fig.11(c) and Fig.11(d), the bonding bridges breaks contained voids before modification. The modified bonding bridges were denser, and the carbon content at point D was higher than point E(Fig.11(d),Table 1). This observation confirmed that

the surface of the modified bonding bridges was enriched with hydrophobic Span-80 and the wettability of the system was good.

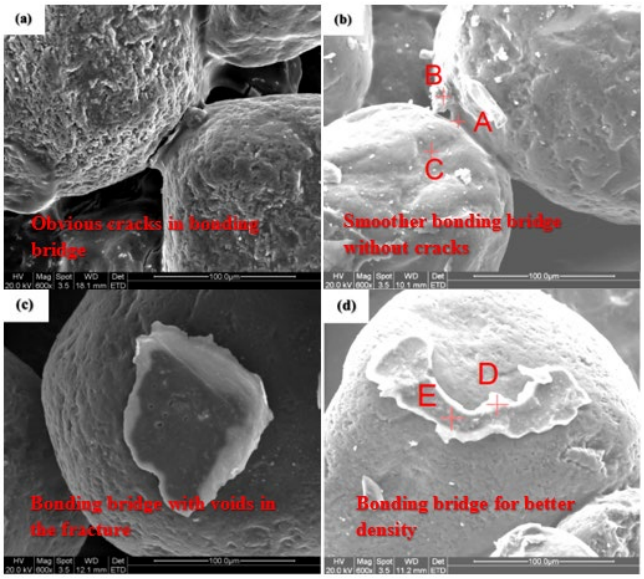

Fig. 11. Bonding bridges in sodium silicate sands before (and after) Span-80 modification: a) Unmodified bonding bridge, b) Modified bonding bridge, c) Fracture of unmodified bonding bridge, d) Fracture of modified bonding bridge

Table 1.
EDS of Span-80 in the bonding bridge and its fracture

	C(Wt%)	O(Wt%)	Na(Wt%)	Mg(Wt%)	Al(Wt%)	Si(Wt%)
Point A	15.78	34.04	06.87		08.22	35.09
Point B	32.57	33.93	07.20	01.05	02.87	22.38
Point C	14.64	30.99	03.88		04.01	46.48
Point D	15.10	31.77	07.26		08.58	37.29
Point E	12.08	29.43	16.55		01.43	40.52

Further analyses of IR spectrum of Span-80 and modified sodium silicate sands with Span-80 were shown in Fig.12, Fig.13 and Table.2. The results revealed that the modified sands were enriched with CH_2 and C=O groups, characteristic of Span-80, with no new groups formed. However, the spectral peaks of groups like O-H and -CH_3 had shifted, which facilitated the integration of Span-80 with the sodium silicate sands and enhanced the moisture resistance of NIRC3DPSSS.

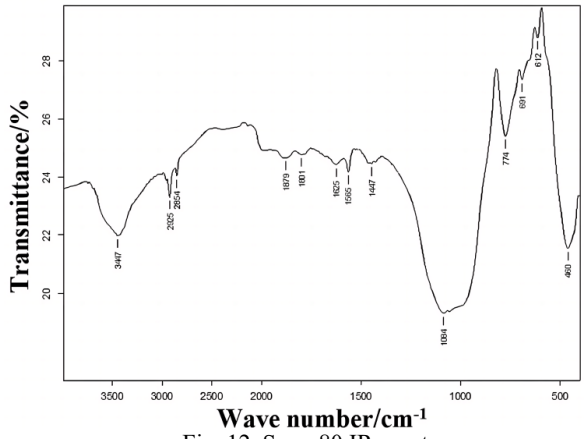

Fig. 12. Span-80 IR spectrum

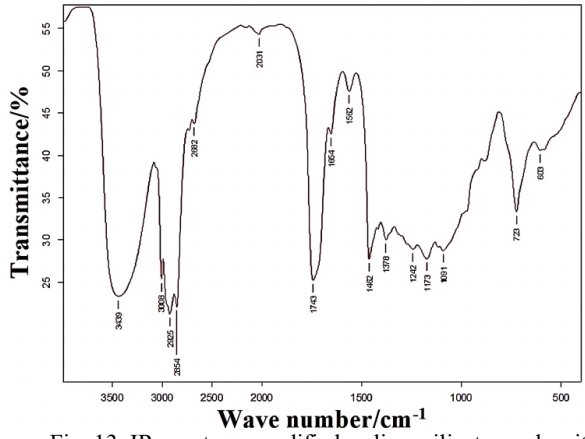

Fig. 13. IR spectrum modified sodium silicate sands with Span-80

Table 2.
IR spectrum and group ownership of modified sodium silicate sands with Span-80

Span-80	**Sodium silicate sands modified with Span-80**	**Functional groups contained in the modified system**
3447	3439	O-H
-	3008	-CH_3
2925	2925	-CH_2-
2854	2854	-CH_2-
-	2682	Water of crystallization
-	2031	C=O
1879	-	-
1801	-	-
-	1743	C=O
1625	1654	Water of crystallization
1565	1562	C-O
1447	1462	O-H
-	1378	C-H

4. Conclusions

During the preparation of sodium silicate sands molds, a photovoltaic-powered NIRC3DPSSS mechanism was utilized. The raw sands were modified with Span-80, resulting in a process that achieved high strength, easy collapsibility, rapid curing, moisture resistance, low energy consumption and environmental friendliness.

1) A new method of NIRC3DPSSS driven by photovoltaic cells was proposed, achieving low sodium silicate addition within 3% with strength reaching 1.5 MPa, but the sands molds had poor moisture resistance.
2) After 4 hours in a humidistat(99%RH), the strength of sands molds containing 2.2% sodium silicate and modified with Span-80 reached 0.95MPa, an increase of 97.9%. In air(80%RH), the strength reached 1.25MPa, an increase of 40.4%. The optimal effect of modification was achieved when Span-80 was 0.066% of the raw sands. The bonding film and bridges protected by Span-80 were more stable, smoother and free of cracks observed by SEM and EDS. The internal structure of the bonding bridges was denser, enhancing the molds strength and moisture resistance.

Acknowledgement

This work was supported by State Key Laboratory of New Textile Materials and Advanced Processing Technologies (No.FZ2021014); the Wuhan Science and Technology Bureau Application Foundation Frontier Project (2022023988065216);the National Natural Science Foundation of China (J2124010,51405348,51575405); the Educational Commission of Hubei Province of China (D20171604); the Hubei Provincial Natural Science Foundation of China (2018CFB673).

References

[1] Nowak, D. (2017). The impact of microwave penetration depth on the process of heating the moulding sand with sodium silicate. *Archives of Foundry Engineering.* 17(4), 115-118. DOI:10.1515/AFE-2017-0140.

[2] Major-Gabryś, K., Hosadyna-Kondracka, M., Puzio, S., Kamińska, J. & Angrecki, M. (2020). The influence of the modified ablation casting on casts properties produced in microwave hardened moulds with hydrated sodium silicate binder. *Archives of Metallurgy and Materials*. 65(1), 497-502. DOI: 10.24425/amm.2020.131753.

[3] Stachowicz, M. (2023). Effectiveness of absorbing microwaves by the multimaterial sodium silicate base sand-PLA (Polylactide) mould wall systems. *Archives of Foundry Engineering.* 23(3), 30-37. DOI: 10.24425/afe.2023.144312.

[4] Halejcio, D. & Major-Gabryś, K. (2024). The use of 3D printed sand molds and cores in the castings production. *Archives of Foundry Engineering.* 24(1), 32-39. DOI:10.24425/afe.2024.149249.

[5] Sachs, E., Cima, M., Williams, P., Brancazio, D. & Cornie, J. (1992). Three dimensional printing: rapid tooling and prototypes directly from a CAD model. *Journal of Engineering for Industry.* 114(4), 481-488. https://doi.org/10.1115/1.2900701.

[6] Li, X.Y., Wu, Y,H. & Zhang, S. (2006). Principle and experimental research of three dimensional printing. *Zhongguo Jixie Gongcheng |(China Mechanical Engineering).* 17(13), 1355-1359. DOI: 10.3321/j.issn:1004-132X.2006.13.009.

[7] Wang, R. (2020). Experimental and numerical study on lunar regolith solar 3D printing for engineering material utilization. *Harbin Institute of Technology.* DOI:10.27061/d.cnki.ghgdu.2020.002094.

[8] Chen, J.Y. (2022). Mechanism, process and properties of the typical silicate products based on solar 3D printing. *Harbin Institute of Technology.* DOI:10.27061/d.cnki.ghgdu.2022.003602.

[9] Jia H., Sun H., Wang H., Wu, Y. & Wang, H. (2021). Scanning strategy in selective laser melting (SLM): a review. *The International Journal of Advanced Manufacturing Technology*. 113(9), 2413-2435. DOI: https://doi.org/10.1007/s00170-021-06810-3.

[10] Ninghui, Z., Jianguo, Y., Yujie, G. & Yi, L. Research and application of rapid solidification methods for sand 3D printing equipment. *China Foundry Machinery & Technology*. 58(5), 66-69. DOI: 10.3969/j.issn.1006-9658.2023.05.014.

[11] Wang, X.R., Li, L., Yuwen, D., Wang, J., Wang, D. & Zhou, Q.Q. (2023). Preparation and application properties of waterborne wax emulsions. *Leather and chemical*. (05), 18-21. DOI:10.3969/j.issn.1674-0939.2023.05.003.

[12] Yang, X.N., Zhang, L., Jin, X., Hong, J., Ran, S. & Zhou, F. (2023). Development of water-soluble composite salt sand cores made by a hot-pressed sintering process. *Archives of Foundry Engineering*. 23(3), 51-58. DOI: 10.24425/afe.2023.146662.

[13] Huafang, W., Wenbang, G. & Jijun, L. (2014). Improve the humidity resistance of sodium silicate sands by ester-microwave composite hardening. *Metalurgija*. 53(4), 455-458.

[14] Li, X.J., Fan, Z.T. & Wang, H.F. (2012). Strength and humidity resistance of sodium silicate sand by ester-microwave composite curing. *Zhuzao/Foundry*. 61(2), 147-151.

[15] Stachowicz, M., Pałyga, Ł. & Kępowicz, D. (2020). Influence of automatic core shooting parameters in hot-box technology on the strength of sodium silicate olivine moulding sands. *Archives of Foundry Engineering.* 20(1), 67-72. DOI: 10.24425/afe.2020.131285.

[16] Zhang, Z.F., Wang, L., Zhang, L.T., Ma, P.F., Lu, B.H. & Du, C. W. (2021). Binder jetting 3D printing process optimization for rapid casting of green parts with high tensile strength. *China Foundry.* 18(4), 335-343. DOI: 10.1007/s41230-021-1057-z.